Nuclear Science and Techniques (2025) 36:176
https://doi.org/10.1007/s41365-025-01764-7

High-resolution neutron spectrum regulation for promoting transuranic isotope production

Qing-Quan Pan[1,2] · Lian-Jie Wang[3] · Bang-Yang Xia[3] · Yun Cai[3] · Xiao-Jing Liu[1,2]

Received: 8 January 2025 / Revised: 27 February 2025 / Accepted: 10 March 2025 / Published online: 7 July 2025
© The Author(s), under exclusive licence to China Science Publishing & Media Ltd. (Science Press), Shanghai Institute of Applied Physics, the Chinese Academy of Sciences, Chinese Nuclear Society 2025

Abstract
A method is proposed for high-resolution neutron spectrum regulation across the entire energy domain. It was applied to in-reactor transuranic isotope production. This method comprises four modules: a neutron spectrum perturbation module, a neutron spectrum calculation module, a neutron spectrum valuation module, and an intelligent optimization module. It makes it possible to determine the optimal neutron spectrum for transuranic isotope production and a regulation scheme to establish this neutron spectrum within the reactor. The state-of-the-art production schemes for ^{252}Cf and ^{238}Pu in the High Flux Isotope Reactor were optimized, improving the yield of ^{252}Cf by 12.16% and that of ^{238}Pu by 7.53–25.84%. Moreover, the proposed optimization schemes only disperse certain nuclides into the targets without modifying the reactor design parameters, making them simple and feasible. The new method achieves efficient and precise neutron spectrum optimization, maximizing the production of transuranic isotopes.

Keywords Californium-252 · Plutonium-238 · Neutron spectrum regulation · Genetic algorithm · High resolution

1 Introduction

Transuranic isotopes [1] are isotopes of elements with atomic numbers greater than uranic (element 92), such as californium-252 (^{252}Cf), curium-242 (^{242}Cm), americium-241 (^{241}Am), and plutonium-238 (^{238}Pu). These isotopes are widely used in industry, agriculture, medicine, and national defense [2]. For example, ^{252}Cf, with its high neutron source intensity and continuous energy spectrum, is used as a neutron source for reactor startup [3]; ^{238}Pu, characterized by its long half-life, high thermal power density, and easy shielding of α-decay, is employed as radioactive heat sources [4], and ^{241}Am, a high-quality low-energy gamma source, is utilized in smoke detectors and isotope thickness gauges [5]. Currently, only the USA and Russia possess stable production capabilities for transuranic isotopes. However, during the past 60 years, the USA has only produced 10.2 g of ^{252}Cf [6]. Therefore, transuranic isotopes are scarce strategic materials.

Transuranic isotopes are primarily produced through reactor irradiation, but this process faces the challenges of low nuclide conversion rates and high production costs [7]. Taking the production of ^{252}Cf through the irradiation of ^{242}Pu as an example, as shown in Fig. 1, this process requires ^{242}Pu to absorb ten neutrons continuously without undergoing fission reactions. Otherwise, all previous efforts would be wasted. However, the nuclide conversion chain consists of neutron-rich nuclides, which are prone to fission reactions, leading to fission losses of up to 99% [8]. Neutrons of different energy regions have different capacities for inducing various nuclear reactions, and regulating the neutron spectrum can control the nuclear reaction process [9]. Therefore, by adjusting the neutron spectrum within the irradiation channel, fission losses can be reduced, and the production

This work was sponsored by the National Natural Science Foundation of China (No. 12305190) and the Lingchuang Research Project of the China National Nuclear Corporation (CNNC).

✉ Qing-Quan Pan
panqingquan@sjtu.edu.cn

1 School of Nuclear Science and Engineering, Shanghai Jiao Tong University, Shanghai 200240, China

2 Shanghai Digital Nuclear Reactor Technology Fusion Innovation Center, Shanghai Jiao Tong University, Shanghai 200240, China

3 Science and Technology on Reactor System Design Technology Laboratory, Nuclear Power Institute of China, Chengdu 610200, China

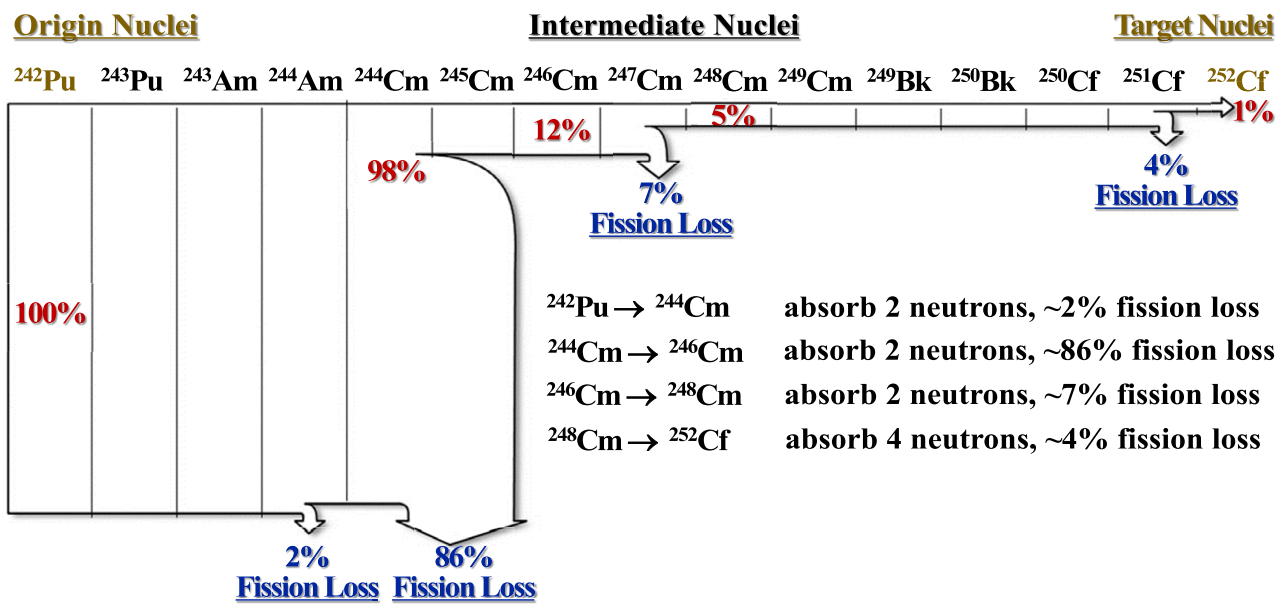

Fig. 1 (Color online) Nuclide chain and fission losses of ^{252}Cf production by irradiated ^{242}Pu

efficiency of transuranic isotopes can be increased by up to 65 times [10]. However, this process faces two challenges: (1) determining the optimal neutron spectrum for transuranic isotope production and (2) determining how to construct the optimal neutron spectrum.

Regarding the first challenge, the research team at Shanghai Jiao Tong University conducted studies to identify the optimal neutron spectrum for transuranic isotope production. (1) *Rapid diagnostic method* [10]: The relationship between production efficiency and neutron spectrum was established, and the concept of energy spectrum total value replaced burnup calculation for efficient evaluation of irradiation schemes. However, this method can only consider the initial neutron spectrum and nuclide composition of the initial target, resulting in theoretical flaws. (2) *Key nuclide analysis method* [11]: The most negative nuclides (key nuclides) during the entire irradiation period were found, and the production efficiency was improved by suppressing the nuclear reactions of these key nuclides. However, this method fails to consider the dynamic evolution of the neutron spectrum and still has theoretical flaws. (3) *Subgroup-burnup and extreme-burnup analysis methods* [12]: The values of neutrons in different energy ranges for transuranic isotope production were quantified, and all nuclides and all neutron spectra throughout the entire irradiation period were considered. However, the results of these two methods are influenced by reactor parameters (neutron flux and irradiation duration), limiting their universal applicability. (4) *Optimal spectrum database* [13]: Genetic algorithms and point burnup calculations were combined to search for the theoretically optimal neutron spectrum under different irradiation durations and neutron fluxes, which comprehensively answers the first question from a scientific perspective.

Regarding the second challenge, neutron spectrum regulation is difficult because neutrons are electrically neutral, unlike charged particles, such as electrons and protons. Current research on this topic is still in its nascent stages and is characterized by four defects: (1) a narrow energy range for neutron spectrum regulation, (2) low spectral resolution during the regulation process, (3) large deviation between the actual and target spectra, and (4) poor universality in terms of the source and target spectra. For example, based on the findings of the first challenge, the research team at Shanghai Jiao Tong University adopted spectrum filtering technology [11] for neutron spectrum regulation, thereby enhancing the production efficiency of transuranic isotopes. However, this method can only reduce the neutron flux at a single energy point or within a narrow energy range, limiting its spectral regulation capabilities. Muhrer [14] proposed the "golden rule" to define the relationship between the neutron moderation effect and the hydrogen content in the moderating material, which can guide the process of neutron moderation. However, the neutron spectrum resolution that can be achieved using this process is low. Scherr and Tsvetkov [15] relied on manual experience to adjust the materials and geometric dimensions of the regulation modules to match the reactor spectrum to the target spectrum. However, this iterative trial-and-error method struggles to ensure the accuracy of the regulation results and is labor intensive. Cao [16]

suggested an inverse correction method for spectrum regulation; however, it is constrained by the low precision of spectrum calculations and the limitations of the regulation modules, which restrict the achievable target spectra. Therefore, technology capable of achieving high-precision and high-universality neutron spectrum regulation across the full energy range with high spectral resolution remains lacking.

A method for high-resolution neutron spectrum regulation across the full energy range is proposed. It can be applied to improve the yield of transuranic isotopes by optimizing the neutron spectrum. The remainder of this article is structured as follows. In Sect. 2, the methods are introduced. The applications are discussed in Sect. 3. Section 4 concludes the article.

2 Methods

2.1 Rapid calculation of neutron spectrum

A genetic algorithm [17] was employed for neutron spectrum optimization. A large number of irradiation schemes are screened, necessitating a rapid algorithm for calculating the neutron spectrum, where a previously proposed method [18] was adopted.

Assuming that a neutron with energy E_i undergoes a nuclear reaction with a non-absorbing nuclide, the energy of the neutron then changes to

$$E_j = \sum_i P_{i,j}(E_i) \cdot E_i, \tag{1}$$

where E_i and E_j represent the neutron energies before and after the reaction, respectively, and $P_{i,j}$ denotes the probability of the energy transfer from E_i to E_j. If the continuous energy is divided into n energy bins, $P_{i,j}$ can be written as an $n \times n$ matrix,

$$\boldsymbol{R}_k = \begin{pmatrix} r_{0,0} & \cdots & \cdots & r_{0,n} \\ \vdots & \ddots & r_{i,j} & \vdots \\ \vdots & \vdots & \ddots & \vdots \\ r_{n,0} & \cdots & \cdots & r_{n,n} \end{pmatrix}, \tag{2}$$

and Eq. (1) can also be rewritten in matrix form,

$$\boldsymbol{V}_1 = \boldsymbol{R}_k \boldsymbol{V}_0, \tag{3}$$

where $\boldsymbol{V}_0$ and $\boldsymbol{V}_1$ represent the neutron spectra before and after the reaction; $\boldsymbol{R}_k$ is the spectrum response matrix for nuclide k; and the matrix element $r_{i,j}$ represents the probability of energy transfer from energy bin i to energy bin j.

To consider absorption reactions, each row of the matrix is normalized,

$$a_i + \sum_{j=1}^{n} r_{i,j} = 1, \tag{4}$$

where a_i is the neutron absorption probability in energy bin i.

Equation (4) makes the sum of each row of $\boldsymbol{R}_k$ less than 1.0, causing the norm of $\boldsymbol{V}_1$ also to be less than 1.0, where Eq. (3) fails to yield a stable neutron spectrum. In this case, $\boldsymbol{V}_0$ is used to supplement the reduction in $\boldsymbol{V}_1$ after each iteration,

$$\boldsymbol{V}_1 = \boldsymbol{R}_k \boldsymbol{V}_0 + \frac{|\boldsymbol{V}_0| - |\boldsymbol{R}_k \boldsymbol{V}_0|}{|\boldsymbol{V}_0|} \boldsymbol{V}_0. \tag{5}$$

To consider the presence of multiple nuclides in a material, the spectrum response matrices of each nuclide are used to form a spectrum response matrix of this material,

$$\boldsymbol{R}_{\text{mat}} = \sum_{k=0}^{n} \boldsymbol{F}_k \boldsymbol{R}_k, \tag{6}$$

where $\boldsymbol{F}_k$ is a diagonal matrix composed of the weights of nuclide k,

$$\boldsymbol{F}_k = \begin{pmatrix} f_{k,1} & & & \\ & f_{k,2} & & \\ & & \ddots & \\ & & & f_{k,n} \end{pmatrix}, \tag{7}$$

where the matrix element $f_{k,i}$ represents the weight of nuclide k in energy bin i. It reflects the importance of nuclide k to the spectrum transfer process in this material,

$$f_{k,i} = \frac{\Sigma_{\text{total}}^{k,i}}{\Sigma_{\text{total}}^{i}}, \tag{8}$$

where $\Sigma_{\text{total}}^{k,i}$ is the macroscopic total cross section of nuclide k in energy bin i and $\Sigma_{\text{total}}^{i}$ is the macroscopic total cross section of the material in energy bin i.

To consider different geometries, the leakage of neutrons is calculated because some neutrons fly out of the system without reaction. The probability p_i of a neutron not undergoing a collision can be derived based on the exponential decay law,

$$p_i = e^{-\Sigma_{\text{total}}^{i} \cdot b}, \tag{9}$$

where b is the distance to the boundary, which is related to the geometric parameters of the system. Then, the spectrum response matrix is revised to

$$\boldsymbol{R}_{\text{real}} = \boldsymbol{R}_k \times (\boldsymbol{I} - \boldsymbol{P}), \tag{10}$$

where $\boldsymbol{R}_{\text{real}}$ is the true spectrum response matrix for the geometry, $\boldsymbol{I}$ is the identity diagonal matrix, and $\boldsymbol{P}$ is a diagonal matrix composed of the non-collision probabilities,

$$\boldsymbol{P} = \begin{pmatrix} p_1 & & & \\ & p_2 & & \\ & & \ddots & \\ & & & p_n \end{pmatrix}. \tag{11}$$

With Eqs. (3), (5), (6), and (10), the output neutron spectrum for any source neutron spectrum under any geometric and material conditions can be calculated rapidly.

2.2 High-resolution spectrum regulation

Equation (8) indicates that the response relationship of neutron spectra is correlated with the isotopic composition of the materials. Therefore, the neutron spectrum can be modulated by altering the isotopic composition within a spatial region. The spectrum response matrices of 423 isotopes were built, and the full energy range was divided into 238 energy bins [19] to enhance the spectral resolution and precision of neutron spectrum regulation.

The source neutron spectrum (n energy bins) is denoted as $\boldsymbol{\psi}_{\text{in}} = \{x_1, x_2, \ldots, x_n\}$, and the output neutron spectrum is denoted as $\boldsymbol{\psi}_{\text{out}} = \{y_1, y_2, \ldots, y_n\}$. A stable output neutron spectrum can be obtained from the iterative convergence of Eq. (3),

$$\boldsymbol{\psi}_{\text{out}} = \sum_{m=1}^{\infty} \phi_m, \tag{12}$$

where $\boldsymbol{\phi}_m$ represents the neutron spectrum after m collisions, which is calculated by

$$\phi_m = \boldsymbol{R}_{\text{real}} \cdot \phi_{m-1} = \boldsymbol{R}_{\text{real}}^2 \cdot \phi_{m-2} = \cdots = \boldsymbol{R}_{\text{real}}^{m-1} \cdot \phi_1 = \boldsymbol{R}_{\text{real}}^{m} \cdot \boldsymbol{\psi}_{\text{in}}. \tag{13}$$

Combining Eqs. (12) and (13), one obtains

$$\boldsymbol{\psi}_{\text{out}} = \sum_{m=1}^{\infty} \phi_m = \boldsymbol{\psi}_{\text{in}} + \boldsymbol{R}_{\text{real}} \cdot \boldsymbol{\psi}_{\text{in}} + \boldsymbol{R}_{\text{real}}^2 \cdot \boldsymbol{\psi}_{\text{in}} + \boldsymbol{R}_{\text{real}}^3 \cdot \boldsymbol{\psi}_{\text{in}} + \cdots = \frac{\boldsymbol{\psi}_{\text{in}}}{\mathrm{I} - \boldsymbol{R}_{\text{real}}}, \tag{14}$$

and simplifying Eq. (14) yields

$$\boldsymbol{\psi}_{\text{out}} = \frac{\boldsymbol{I}}{\boldsymbol{I} - \boldsymbol{R}_{\text{real}}} \cdot \boldsymbol{\psi}_{\text{in}} = \boldsymbol{A} \cdot \boldsymbol{\psi}_{\text{in}}, \tag{15}$$

where $\boldsymbol{A}$ is a spectral matrix that transforms the source neutron spectrum into the output neutron spectrum. Many matrices satisfy Eq. (15), for example,

$$\begin{bmatrix} a_{11} & a_{12} & \cdots & a_{1n} \\ a_{21} & a_{22} & \cdots & a_{2n} \\ \vdots & \vdots & \ddots & \vdots \\ a_{n1} & a_{n2} & \cdots & a_{nn} \end{bmatrix} \begin{bmatrix} x_1 \\ x_2 \\ \vdots \\ x_n \end{bmatrix} = \begin{bmatrix} \frac{x_1 \cdot y_1}{\sum_1^n x_i^2} & \frac{x_2 \cdot y_1}{\sum_1^n x_i^2} & \cdots & \frac{x_n \cdot y_1}{\sum_1^n x_i^2} \\ \frac{x_1 \cdot y_2}{\sum_1^n x_i^2} & \frac{x_2 \cdot y_2}{\sum_1^n x_i^2} & \cdots & \frac{x_n \cdot y_2}{\sum_1^n x_i^2} \\ \vdots & \vdots & \ddots & \vdots \\ \frac{x_1 \cdot y_n}{\sum_1^n x_i^2} & \frac{x_2 \cdot y_n}{\sum_1^n x_i^2} & \cdots & \frac{x_n \cdot y_n}{\sum_1^n x_i^2} \end{bmatrix} \begin{bmatrix} x_1 \\ x_2 \\ \vdots \\ x_n \end{bmatrix} = \begin{bmatrix} y_1 \\ y_2 \\ \vdots \\ y_n \end{bmatrix}. \tag{16}$$

If matrix $\boldsymbol{A}$ can be constructed with a certain isotopic composition of these 423 nuclides, then the high-resolution neutron spectrum is achieved without any deviation. However, because the full energy range has been divided into 238 energy bins for high resolution, $\boldsymbol{A}$ is a 238×238 matrix, making the construction of $\boldsymbol{A}$ quite challenging. $\boldsymbol{A}$ cannot be obtained solely based on these 423 matrices. Instead, one can use only these 423 matrices to construct a matrix-approximating matrix $\boldsymbol{A}$.

2.3 Yield maximum with optimal spectrum regulation

Previous studies have demonstrated that transuranic isotope production can be improved greatly by neutron spectrum optimization and have provided the importance curves that quantify the values of neutrons in various energy bins for the production of transuranic isotopes [12], as shown in Fig. 2. To determine the optimal neutron spectrum further, a genetic algorithm was employed to build an optimal spectrum database that provides the optimal neutron spectra under different neutron fluxes and irradiation durations [13]. The theoretical maximum yields of ^{238}Pu under different irradiation conditions are shown in Fig. 3. Therefore, once this optimal neutron spectrum is constructed within the target, the yields of transuranic isotopes can be maximized.

To construct the optimal neutron spectrum inside the target based on an initial irradiation scheme, it is necessary to build a spectrum response matrix that converts the initial neutron spectrum into the optimal one. However, it is impossible to construct the optimal neutron spectrum using only the spectrum response matrices of these 423 nuclides. Therefore, a genetic algorithm is employed to search for the optimal proportions of these 423 nuclides, such that the neutron spectrum inside the target is closest to the optimal one, thereby maximizing the yields of transuranic isotopes. As shown in Fig. 4, the specific calculation process is as follows.

(1) Constructing the initial population for the genetic algorithm: Various nuclides are randomly added to the target, constructing different neutron spectrum regulation schemes. Assuming that there are originally i types of nuclide in the target, the spectrum response matrix inside the target at this time is

$$\boldsymbol{R}_{\text{real}} = \sum_{k=0}^{i} \boldsymbol{F}_k \boldsymbol{R}_k \times (\boldsymbol{I} - \boldsymbol{P}), \tag{17}$$

and the spectrum response matrix inside the target is changed after j new types of nuclides are added to the target,

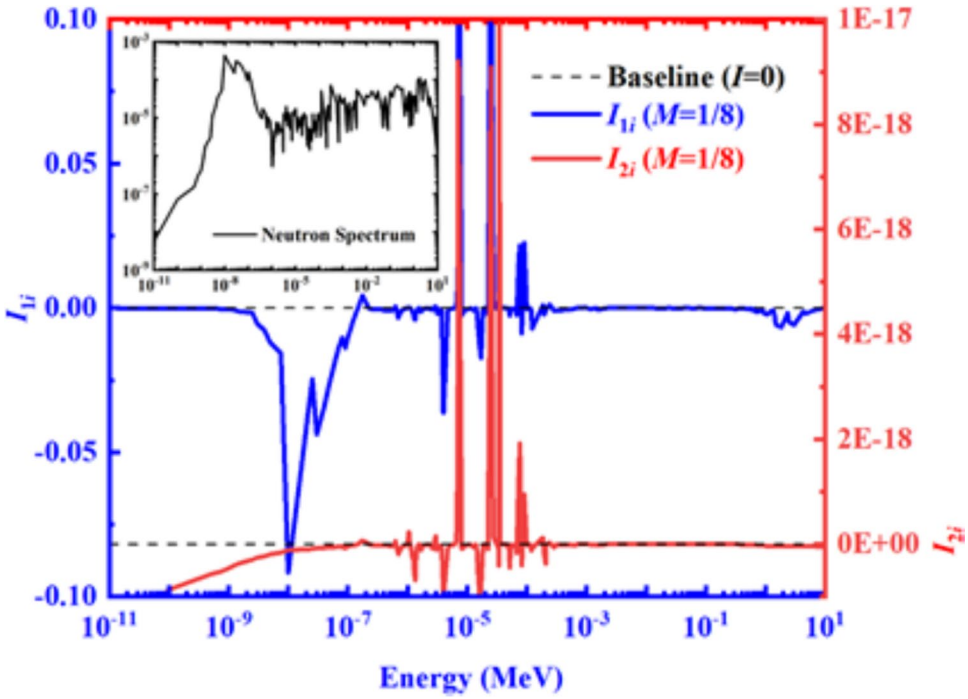

Fig. 2 Value of neutrons in each energy region for ^{252}Cf production [12]

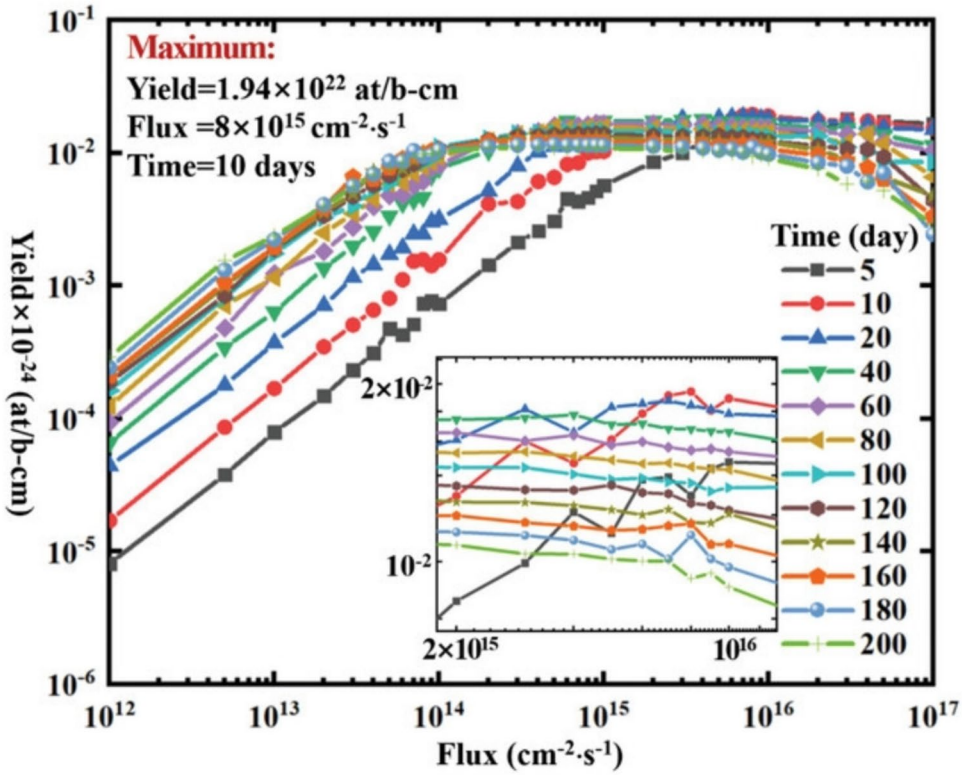

Fig. 3 Maximum yields under different flux levels and irradiation durations [13]

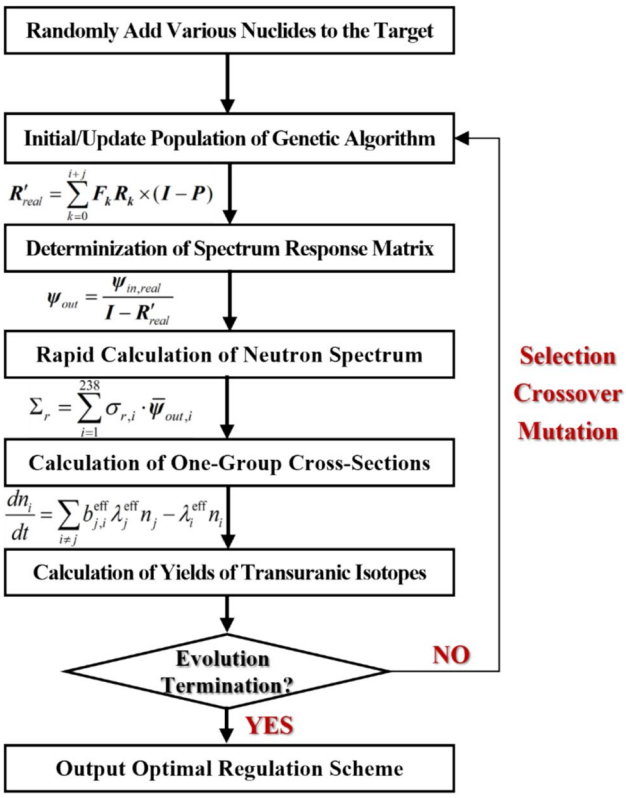

Fig. 4 Flowchart for searching the optimal neutron spectrum

$$R'_{\text{real}} = \sum_{k=0}^{i+j} F_k R_k \times (I - P). \tag{18}$$

(2) Calculation of the neutron spectrum inside the target: In the case of a known fixed source term, the neutron spectrum can be directly calculated using Eq. (14). However, because the incident neutron spectrum of the irradiation channel also changes after the target material is modified, the incident neutron spectrum must be updated according to the nuclide composition of the target. Linear interpolation is used to provide the incident neutron spectra for various nuclide compositions inside the target, as shown in Fig. 5.

To accomplish this, one first must determine two initial source terms: the incident neutron spectra $\psi_{\text{in},0}$ and $\psi_{\text{in},\infty}$ when the cross sections of the material in the irradiation channel are zero and infinity, respectively. Then, the non-collision probability P in Eq. (9) is used as the interpolation factor to calculate the incident neutron spectrum for different nuclide compositions inside the target,

$$\psi_{\text{in,real}} = (I - P) \times \psi_{\text{in},0} + P \times \psi_{\text{in},\infty}. \tag{19}$$

After the spectrum response matrix of the target and incident initial neutron spectrum are determined, the

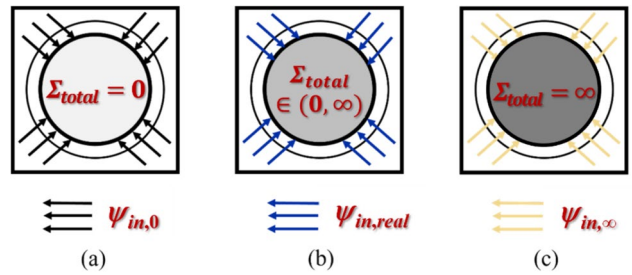

Fig. 5 Schematic diagram for determining the incident neutron spectra

neutron spectrum inside the target can be quickly calculated using the following equation:

$$\psi_{\text{out}} = \frac{\psi_{\text{in,real}}}{I - R'_{\text{real}}}. \tag{20}$$

(3) Calculating the yields of transuranic isotopes: To meet the high computational demand of the genetic algorithm, the yields of transuranic isotopes are calculated by solving the burnup equation [20, 21],

$$\frac{\mathrm{d}n_i}{\mathrm{d}t} = \sum_{i \neq j} b_{j,i}^{\text{eff}} \lambda_j^{\text{eff}} n_j - \lambda_i^{\text{eff}} n_i, \tag{21}$$

where n_i is the density of the ith nuclide, λ_i^{eff} is the effective decay constant of the ith nuclide, and $b_{i,j}^{\text{eff}}$ is the branching ratio for the transmutation of the ith nuclide to the jth nuclide. In addition, λ_i^{eff} and $b_{i,j}^{\text{eff}}$ can be calculated from the following formula,

$$\begin{cases} \lambda_i^{\text{eff}} = \lambda_i + \phi \sum_j \sigma_{i,j} \\ b_{i,j}^{\text{eff}} = (b_{i,j}\lambda_i + \sigma_{i,j}\phi)/\lambda_i^{\text{eff}} \end{cases}, \tag{22}$$

where λ_i is the decay constant of the ith nuclide, ϕ is the neutron flux, and $\sigma_{i,j}$ is the one-group cross section where the reaction of the ith nuclide generates the jth nuclide.

The one-group macroscopic cross sections $\sum_{\text{r}}$ of a neutron spectrum needed by the point burnup calculation are calculated by

$$\Sigma_{\text{r}} = \sum_{i=1}^{238} \sigma_{\text{r},i} \cdot \overline{\psi}_{\text{out},i}, \tag{23}$$

where the subscript i represents an energy bin; subscript r represents a reaction type, $\overline{\psi}_{\text{out},i}$ represents the normalized output neutron spectrum, and σ represents the grouped microscopic cross section.

(4) Performing evolutionary operations on the population: With the yield of transuranic isotopes as the

optimization objective, the population is screened, crossed, and mutated to obtain a new population. Step (2) is then repeated until the evolution of the population is completed.

(5) Outputting the optimal neutron spectrum regulation scheme: The optimal neutron spectrum regulation scheme is described in terms of the types and proportions of nuclides added to the target, along with the yields of transuranic isotopes under this optimal scheme and its enhancement effect compared with the original production scheme.

The nuclear data, such as decay data, cross-section data, and fission yield data required for the neutron spectrum and burnup calculation in this study, all originate from ENDF/B-VII.1 [9]. The spatial self-shielding effect of the target can be considered during neutron energy spectrum calculation.

3 Applications

3.1 State-of-the-art irradiation scheme

The High Flux Isotope Reactor (HFIR) [22] is currently the primary facility for transuranic isotope production, accounting for 70% of the global ^{252}Cf supply. HFIR has a steady-state neutron thermal flux of 2.5×10^{15} cm^{-2} s^{-1} and a refueling cycle of 25 days. HFIR and the target are modeled using the RMC code [23–25], as shown in Fig. 6.

The volumetric neutron spectrum inside the target is changed by adding various nuclides to it. The state-of-the-art irradiation scheme (called "SOTA") employs a target with a diameter of 5 mm, whereas the diameter of the reactor is 110 cm, resulting in an extremely narrow range for neutron spectrum regulation. For comparison, an alternative irradiation scheme (called "ALTER") was envisioned in which targets are placed throughout the entire neutron flux trap. In this hypothetical scenario, the diameter of the target is 12.6 cm, which has a larger range of neutron spectrum regulation than SOTA. Monte Carlo simulations were employed to obtain the incident neutron spectra when the cross sections of the target are zero and infinity. Furthermore, based on Eqs. (19) and (20), the adjustable range of the neutron spectrum for ^{252}Cf production using the two irradiation schemes was calculated, as shown in Fig. 7. The average relative deviation (*Ave*.Re) of the neutron spectrum is used to measure its adjustable range,

$$\text{Ave.Re} = \sum_{i=1}^{238} \left| \frac{\phi_{0,i} - \phi_{\infty,i}}{\phi_{\infty,i}} \right| \Big/ 238, \tag{24}$$

where $\phi_{0,i}$ and $\phi_{\infty,i}$ are the volumetric neutron spectra inside the target when the cross sections of the target are zero and infinity, respectively.

Table 1 presents the Ave.Re of the incident neutron spectra, the volumetric neutron spectrum inside the target for

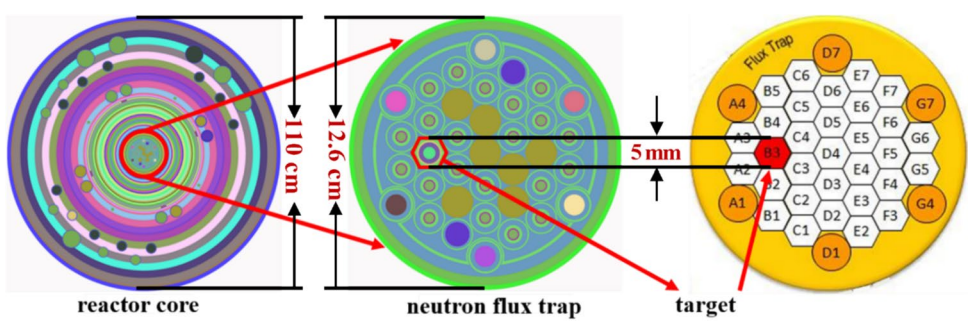

Fig. 6 (Color online) Modeling diagram of HFIR and the target

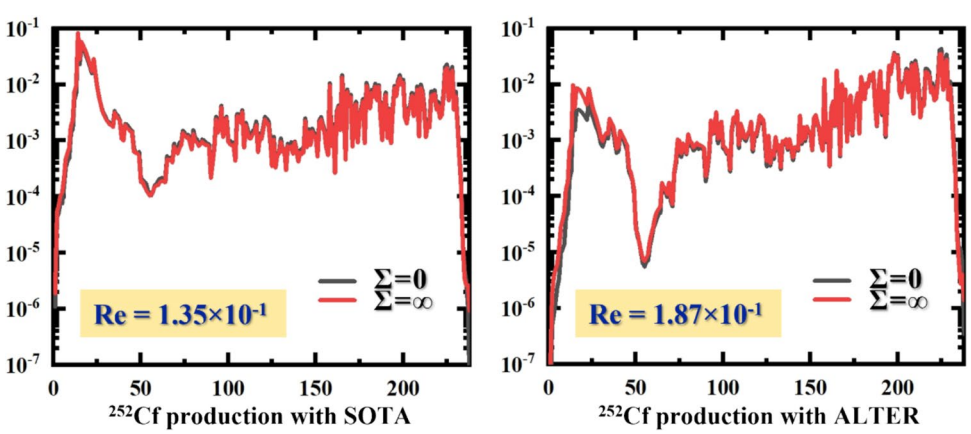

Fig. 7 Adjustable range of the neutron spectrum for ^{252}Cf production

Table 1 Ave.Re of the neutron spectra

Scheme	Incident	^{252}Cf	^{238}Pu (^{237}Np)	^{238}Pu (^{241}Am)
SOTA	1.38×10^{-1}	1.35×10^{-1}	7.53×10^{-2}	1.01×10^{-1}
ALTER	2.14×10^{-1}	1.87×10^{-1}	2.22×10^{-1}	2.30×10^{-1}

^{252}Cf and ^{238}Pu (two types of target) production when the cross sections of the target are zero and infinity.

As shown in Fig. 7 and Table 1, the range for neutron spectrum regulation is small, which makes neutron spectrum optimization extremely difficult. The HFIR irradiation scheme of transuranic isotope production, which is currently the optimal irradiation scheme available, is chosen as the initial approach in this study. If the research presented in this paper can further enhance these state-of-the-art irradiation schemes through neutron spectrum regulation, the significance of our work can be demonstrated.

In the subsequent analysis, the neutron spectrum within the flux trap and target is adopted as the starting point for neutron spectrum regulation. The neutron flux for point burnup calculations is 2.5×10^{15} cm^{-2}·s^{-1}, with a burnup time of 25 days, which is divided into 10 subburnup steps. During the calculation process, the genetic algorithm is first used to search for and identify the 20 most important nuclides for enhancing the yield of transuranic isotopes. The concentrations of these 20 nuclides are then optimized. Hence, in the next section, the addition of these 20 most important nuclides for yield improvement is discussed.

3.2 Volumetric neutron spectrum regulation for ^{252}Cf production

The target for ^{252}Cf production is a mixture of plutonium, americium, and curium [26, 27], whose nuclide components are listed in Table 2. The calculation procedure outlined in Fig. 4 was used to optimize the neutron spectrum for the SOTA and ALTER irradiation schemes.

For the SOTA irradiation scheme, the yield of ^{252}Cf after 25-day irradiation of this target in HFIR is 1.33×10^{18} atom/cm^3. After the nuclides listed in Table 3 are added to the target, a maximum yield of 1.49×10^{18} atom/cm^3 can be achieved, a 12.16% increase compared with the original SOTA irradiation scheme.

For the ALTER irradiation scheme, the yield of ^{252}Cf after 25-day irradiation of this target in HFIR is 1.15×10^{17} atom/cm^3. After the nuclides listed in Table 4 are added to the target, a maximum yield of 1.77×10^{17} atom/cm^3 can be achieved, which is a 54.54% increase compared with the original ALTER irradiation scheme.

The nuclides listed in Tables 3 and 4 are added to the target by dispersion, with the density of the added nuclides not exceeding 1% of the initial nuclide density of the target.

Table 2 Nuclide components of the target for ^{252}Cf production

Isotopes	Number density (atom/cm^3)	Isotopes	Number density (atom/cm^3)	Isotopes	Number density (atom/cm^3)
^{16}O	3.68×10^{21}	^{56}Fe	7.66×10^{19}	^{242m}Am	1.33×10^{17}
^{27}Al	4.72×10^{22}	^{57}Fe	1.74×10^{18}	^{243}Am	1.18×10^{20}
^{40}Ca	7.38×10^{19}	^{58}Fe	2.27×10^{17}	^{242}Cm	3.71×10^{16}
^{42}Ca	4.69×10^{17}	^{238}Pu	1.86×10^{18}	^{243}Cm	2.61×10^{17}
^{43}Ca	9.56×10^{16}	^{239}Pu	1.66×10^{17}	^{244}Cm	3.60×10^{20}
^{44}Ca	1.44×10^{18}	^{240}Pu	3.51×10^{19}	^{245}Cm	8.44×10^{18}
^{46}Ca	2.65×10^{15}	^{241}Pu	1.12×10^{16}	^{246}Cm	1.11×10^{21}
^{48}Ca	1.19×10^{17}	^{242}Pu	4.63×10^{17}	^{247}Cm	3.14×10^{19}
^{54}Fe	5.06×10^{18}	^{241}Am	3.29×10^{19}	^{248}Cm	2.46×10^{21}

Table 3 Nuclei additions for the SOTA irradiation scheme of ^{252}Cf production

Isotopes	Number density (atom/cm^3)	Isotopes	Number density (atom/cm^3)	Isotopes	Number density (atom/cm^3)
^{1}H	5.14×10^{20}	^{73}Ge	5.25×10^{20}	^{140}La	4.93×10^{20}
^{9}Be	4.51×10^{20}	^{74}Ge	5.04×10^{20}	^{200}Hg	4.45×10^{20}
^{36}Ar	5.20×10^{20}	^{101}Ru	5.20×10^{20}	^{204}Hg	4.72×10^{20}
^{38}Ar	4.88×10^{20}	^{105}Ru	4.45×10^{20}	^{206}Pb	5.25×10^{20}
^{58}Ni	5.25×10^{20}	^{102}Pd	5.14×10^{20}	^{208}Pb	5.20×10^{20}
^{59}Ni	1.06×10^{19}	^{106}Pd	5.25×10^{20}	^{209}Bi	5.25×10^{20}
^{65}Cu	5.09×10^{20}	^{136}Ce	5.09×10^{20}		

Table 4 Nuclei additions for the ALTER irradiation scheme of ^{252}Cf production

Isotopes	Number density (atom/cm^3)	Isotopes	Number density (atom/cm^3)	Isotopes	Number density (atom/cm^3)
^{1}H	1.59×10^{19}	^{12}C	5.25×10^{20}	^{33}S	5.14×10^{20}
^{2}H	4.72×10^{20}	^{15}N	4.56×10^{20}	^{34}S	4.98×10^{20}
^{3}H	4.93×10^{20}	^{17}O	4.83×10^{20}	^{36}S	5.20×10^{20}
^{4}He	4.77×10^{20}	^{28}Si	4.88×10^{20}	^{37}Cl	5.25×10^{20}
^{7}Li	4.77×10^{20}	^{29}Si	4.56×10^{20}	^{40}Ar	5.20×10^{20}
^{9}Be	4.35×10^{20}	^{30}Si	5.20×10^{20}		
^{11}B	5.04×10^{20}	^{32}S	4.51×10^{20}		

After the addition of the nuclides, the density of the original nuclides in the target decreases accordingly. Meanwhile, in this study, a high-resolution neutron spectrum regulation method, achieved by adjusting the proportions of these 423 nuclides within a certain spatial region, was developed. Theoretically, the more the nuclides that can be used for neutron spectrum regulation, the higher the regulation capability. However, many nuclides are unstable and extremely expensive, which makes them difficult to use in practical

Table 5 Nuclide components of the targets for ^{238}Pu production

AmO_2		NpO_2	
Isotopes	Number density (atom/cm^3)	Isotopes	Number density (atom/cm^3)
^{16}O	5.11×10^{22}	^{16}O	4.97×10^{22}
^{241}Am	2.55×10^{22}		
^{242}Am	2.04×10^{17}	^{237}Np	2.49×10^{22}
^{243}Am	1.06×10^{19}		

Table 6 Nuclei additions for the SOTA scheme (AmO_2) of ^{238}Pu production

Isotopes	Number density (atom/cm^3)	Isotopes	Number density (atom/cm^3)	Isotopes	Number density (atom/cm^3)
^{184}W	7.43×10^{20}	^{205}Ti	7.51×10^{20}	^{226}Ra	7.13×10^{20}
^{198}Hg	7.28×10^{20}	^{204}Pb	6.74×10^{20}	^{225}Ac	7.28×10^{20}
^{200}Hg	7.28×10^{20}	^{206}Pb	7.36×10^{20}	^{230}Th	7.59×10^{20}
^{201}Hg	7.51×10^{20}	^{207}Pb	7.59×10^{20}	^{232}Th	7.59×10^{20}
^{202}Hg	7.43×10^{20}	^{208}Pb	7.51×10^{20}	^{234}Th	7.28×10^{20}
^{204}Hg	7.28×10^{20}	^{209}Bi	7.13×10^{20}		
^{203}Ti	7.59×10^{20}	^{224}Ra	7.13×10^{20}		

engineering applications. Therefore, it is recommended that readily available nuclides or natural elements be adopted to develop neutron spectrum regulation schemes in practical engineering.

3.3 Volumetric neutron spectrum regulation for ^{238}Pu production

^{238}Pu is produced by the in-reactor irradiation of americium-241 (^{241}Am) [28, 29] or neptunium-237 (^{237}Np) [30, 31], with the nuclide components of the targets listed in Table 5. Experience has shown that the in-reactor irradiation of ^{237}Np facilitates a higher yield of ^{238}Pu, whereas the in-reactor irradiation of ^{241}Am facilitates a higher abundance of ^{238}Pu. Therefore, these two irradiation methods are currently the practical solutions adopted, and analyses of both methods were conducted.

3.3.1 In-reactor irradiation of ^{241}Am

For the SOTA irradiation scheme, the yield of ^{238}Pu after 25-day irradiation of the AmO_2 target in HFIR is 3.11×10^{20} atom/cm^3. After the nuclides listed in Table 6 are added to the target, a maximum yield of 3.92×10^{20} atom/cm^3 can be achieved, a 25.84% increase compared with the original SOTA irradiation scheme.

Table 7 Nuclei additions for the ALTER scheme (AmO_2) of ^{238}Pu production

Isotopes	Number density (atom/cm^3)	Isotopes	Number density (atom/cm^3)	Isotopes	Number density (atom/cm^3)
^{164}Er	7.51×10^{20}	^{202}Hg	7.13×10^{20}	^{208}Pb	7.05×10^{20}
^{168}Er	7.59×10^{20}	^{204}Hg	7.59×10^{20}	^{209}Bi	7.05×10^{20}
^{180}Hf	7.20×10^{20}	^{203}Ti	7.13×10^{20}	^{226}Ra	7.05×10^{20}
^{184}W	7.36×10^{20}	^{205}Ti	7.43×10^{20}	^{230}Th	7.13×10^{20}
^{198}Hg	6.90×10^{20}	^{204}Pb	7.28×10^{20}	^{232}Th	7.28×10^{20}
^{200}Hg	7.51×10^{20}	^{206}Pb	6.82×10^{20}		
^{201}Hg	7.43×10^{20}	^{207}Pb	7.36×10^{20}		

Table 8 Nuclei additions for the SOTA scheme (NpO_2) of ^{238}Pu production

Isotopes	Number density (atom/cm^3)	Isotopes	Number density (atom/cm^3)	Isotopes	Number density (atom/cm^3)
^{170}Er	7.38×10^{20}	^{201}Hg	7.30×10^{20}	^{207}Pb	7.08×10^{20}
^{180}Hf	6.78×10^{20}	^{202}Hg	7.38×10^{20}	^{208}Pb	6.33×10^{20}
^{180}W	6.93×10^{20}	^{204}Hg	6.70×10^{20}	^{209}Bi	6.63×10^{20}
^{184}W	7.38×10^{20}	^{203}Ti	6.56×10^{20}	^{224}Ra	7.30×10^{20}
^{186}W	6.70×10^{20}	^{205}Ti	7.15×10^{20}	^{232}Th	7.23×10^{20}
^{198}Hg	7.30×10^{20}	^{204}Pb	6.85×10^{20}		
^{200}Hg	6.93×10^{20}	^{206}Pb	6.85×10^{20}		

For the ALTER irradiation scheme, the yield of ^{238}Pu after 25-day irradiation of the AmO_2 target in HFIR is 1.14×10^{19} atom/cm^3. After the nuclides listed in Table 7 are added to the target, a maximum yield of 2.08×10^{19} atom/cm^3 can be achieved, an 81.83% increase compared with the original ALTER irradiation scheme.

3.3.2 In-reactor irradiation of ^{237}Np

For the SOTA irradiation scheme, the yield of ^{238}Pu after 25-day irradiation of the NpO_2 target in HFIR is 2.99×10^{21} atom/cm^3. After the nuclides listed in Table 8 are added to the target, a maximum yield of 3.21×10^{21} atom/cm^3 can be achieved, a 7.53% increase compared with the original SOTA irradiation scheme.

For the ALTER irradiation scheme, the yield of ^{238}Pu after 25-day irradiation of the NpO_2 target in HFIR is 2.56×10^{20} atom/cm^3. After the nuclides listed in Table 9 are added to the target, a maximum yield of 4.32×10^{20} atom/cm^3 can be achieved, a 68.74% increase compared with the original ALTER irradiation scheme.

Table 9 Nuclei additions for the ALTER scheme (NpO_2) of ^{238}Pu production

Isotopes	Number density (atom/cm^3)	Isotopes	Number density (atom/cm^3)	Isotopes	Number density (atom/cm^3)
^{146}Nd	7.23×10^{20}	^{200}Hg	6.93×10^{20}	^{206}Pb	5.66×10^{20}
^{150}Nd	6.63×10^{20}	^{201}Hg	7.23×10^{20}	^{207}Pb	7.30×10^{20}
^{160}Gd	7.38×10^{20}	^{202}Hg	6.93×10^{20}	^{208}Pb	7.08×10^{20}
^{168}Er	6.26×10^{20}	^{204}Hg	7.38×10^{20}	^{209}Bi	7.30×10^{20}
^{180}Hf	6.78×10^{20}	^{203}Ti	7.23×10^{20}	^{226}Ra	6.85×10^{20}
^{184}W	6.93×10^{20}	^{205}Ti	7.30×10^{20}	^{232}Th	6.70×10^{20}
^{198}Hg	7.38×10^{20}	^{204}Pb	7.38×10^{20}		

3.4 Comparison and analyses

The yields of these irradiation schemes are compared in Table 10, showing that the volumetric neutron spectrum regulation method proposed can enhance the production of transuranic isotopes. Even for the state-of-the-art irradiation schemes that are currently optimal, one can still improve their efficiencies. Furthermore, the spectrum optimization schemes proposed are simple and feasible, requiring only the dispersion of various nuclides inside the target without the need to modify reactor design or irradiation channel parameters, making them highly practical for engineering applications.

A comparison between the SOTA irradiation scheme and the ALTER irradiation scheme reveals the following conclusions. (1) The SOTA irradiation scheme consistently outperforms the ALTER irradiation scheme, demonstrating the significance of neutron spectrum regulation for transuranic isotope production. (2) The larger the range for neutron spectrum regulation, the more pronounced the promotion in enhancing transuranic isotope production. Therefore, the volumetric neutron spectrum regulation method proposed can identify and construct an optimal neutron spectrum within a limited range. The calculated results provided only cover a narrow range and fail to reflect the overall physical process. In this study, only the effectiveness of this regulation scheme and its technical value are emphasized, without delving into its physical significance in detail. If further increasing the production of transuranic isotopes is required, merely altering the nuclide composition of the target is insufficient. At this point, modifications to the reactor design are necessary to broaden the regulation range of the neutron spectrum within the irradiation channels. This will be explored in planned future research.

4 Conclusion

Transuranic isotopes are scarce strategic materials primarily produced through the in-reactor irradiation of targets; however, they face the challenge of low production efficiency. Optimizing the volumetric neutron spectrum inside the target can enhance the production of transuranic isotopes. A neutron spectrum regulation method was proposed to construct the optimal volumetric neutron spectrum inside the target and apply this method to producing transuranic isotopes, improving their production efficiency.

The new method utilizes a genetic algorithm to search for the optimal neutron spectrum regulation scheme, which is divided into four modules. (1) Neutron spectrum perturbation module: This module alters the neutron spectrum inside the target by dispersing various nuclides throughout it, thereby constructing diverse neutron spectra. (2) Neutron spectrum calculation module: Leveraging the spectrum response matrices, this module swiftly obtains the neutron spectrum inside the target on a timescale of seconds. (3) Neutron spectrum valuation module: Employing the burnup calculation method, this module obtains the yield of transuranic isotopes under various neutron spectra, evaluating the fitness of each scheme. (4) Intelligent optimization module: Based on the selection, crossover, and mutation operations of the genetic algorithm, this module evolves the neutron spectrum regulation schemes to determine the optimal one.

Optimizations were performed starting from the production schemes of the HFIR. The production schemes for ^{252}Cf and ^{238}Pu were optimized. The optimized schemes enhance the production efficiency of ^{252}Cf by 12.16% and increase the production efficiencies of ^{238}Pu by 25.84% and 7.53%. Because these schemes are currently the optimal ones available, these efficiency improvements demonstrate the effectiveness of the proposed approach. Furthermore, the neutron

Table 10 Comparison of irradiation schemes

	Scheme	Original (atom/cm^3)	Optimal (atom/cm^3)	Promotion (%)
SOTA	^{252}Cf	1.33×10^{18}	1.49×10^{18}	12.16
	^{238}Pu (^{241}Am)	3.11×10^{20}	3.92×10^{20}	25.84
	^{238}Pu (^{237}Np)	2.99×10^{21}	3.21×10^{21}	7.53
ALTER	^{252}Cf	1.15×10^{17}	1.77×10^{17}	54.54
	^{238}Pu (^{241}Am)	1.14×10^{19}	2.08×10^{19}	81.83
	^{238}Pu (^{237}Np)	2.56×10^{20}	4.32×10^{20}	68.74

spectrum was optimized solely by dispersing nuclides within the target, without modifying the reactor design, which is an advantage from the engineering viewpoint. However, many nuclides are unstable and extremely expensive, which makes them difficult to use in practical engineering applications. Therefore, it is recommended that readily available nuclides or natural elements be adopted to develop neutron spectrum regulation schemes in practical engineering.

Author contributions Q. Pan contributed to the writing, concept, calculation, analysis, and supervision; L. Wang, B. Xia, Y. Cai, X. Liu contributed to review and funding.

Data availability The data that support the findings of this study are openly available in Science Data Bank at https://cstr.cn/31253.11.sciencedb.j00186.00729 and https://doi.org/10.57760/sciencedb.j00186.00729

Declarations

Conflict of interest The authors declare that they have no competing interests.

References

1. S.M. Robinson, D.E. Benker, E.D. Collins et al., Production of Cf-252 and other transplutonium isotopes at Oak Ridge National Laboratory. Radiochim. Acta **108**(9), 737–746 (2020). https://doi.org/10.1515/ract-2020-0008
2. O. Artun, Production of energetic ^{232}U, ^{236}Pu, ^{238}Pu, ^{242}Cm, ^{248}Bk, ^{250}Cf, ^{252}Cf and ^{252}Es radioisotopes for use as nuclear battery in thin targets via particle accelerators. Appl. Radiat. Isot. **166**, 109337 (2020). https://doi.org/10.1016/j.apradiso.2020.109337
3. R.C. Martin, J.B. Knauer, P.A. Balo, Production, distribution and application of Californium-252 neutron sources. Appl. Radiat. Isot. **53**, 785–792 (2000). https://doi.org/10.1016/S0969-8043(00)00214-1
4. J.U. Klaehn, D.M. Miller, B.J. Gross et al., Initial phase of Pu-238 production in Idaho National Laboratory. Appl. Radiat. Isot. **169**, 109517 (2021). https://doi.org/10.1016/j.apradiso.2020.109517
5. D. Malain, P. Kanchana, Evaluation of radiation safety for ionization chamber smoke detectors containing Am-241. J. Phys. Conf. Ser. **1285**, 012047 (2019). https://doi.org/10.1088/1742-6596/1285/1/012047
6. E. Collins, J. Ezold, R. Wham et al., US Heavy Actinide Production at Oak Ridge National Laboratory–Ongoing Actinide Partitioning and Transmutation Programs, in *Proceedings of the Sixteenth Information Exchange Meeting on Actinide and Fission Product Partitioning and Transmutation (IEMPT),* Saint Petersburg, Russia, Jun 24, 2020–Jul 1, 2020. https://www.osti.gov/servlets/purl/1992753
7. S. Hogle, G.I. Maldonado, C. Alexander, Increasing transcurium production efficiency through directed resonance shielding. Ann. Nucl. Energy **60**, 267–273 (2013). https://doi.org/10.1016/j.anucene.2013.05.018
8. S. Hogle, Optimization of transcurium isotope production in the High Flux Isotope Reactor. Doctoral Dissertation, University of Tennessee, Knoxville (2012). https://trace.tennessee.edu/utk_graddiss/1529/
9. M.B. Chadwick, M. Herman, P. Oblozinsky et al., ENDF/B-VII.1 Nuclear data for science and technology: cross sections, covariances, fission product yields and decay data. Nucl. Data Sheets **112**(12), 2887–2996 (2011). https://doi.org/10.1016/j.nds.2011.11.002
10. Q. Pan, Q. Zhao, L. Wang et al., Rapid diagnosis method for transplutonium isotopes production in high flux reactor. Nucl. Sci. Tech. **34**, 44 (2023). https://doi.org/10.1007/s41365-023-01185-4
11. Q. Zhao, Q. Pan, L. Wang et al., Neutron spectrum optimization for Cf-252 production based on key nuclides analysis. Radiat. Phys. Chem. **214**, 111294 (2024). https://doi.org/10.1016/j.radphyschem.2023.111294
12. Q. Pan, X. Liu, Y. Xia et al., Spectrum importance model for heavy nuclei synthesis in reactors: Taking ^{252}Cf as an example. Nucl. Eng. Technol. **57**(6), 103426 (2025). https://doi.org/10.1016/j.net.2024.103426
13. Q. Pan, X. Liu, Y. Cai, Optimal irradiation spectrum database for ^{238}Pu production. Adv. Sci. **12**, 10995 (2024). https://doi.org/10.1002/ADVS.202410995
14. Q. Muhrer, Urban legends of thermal moderator design. Nucl. Instrum. Methods Phys. Res. A **664**(1), 38–47 (2012). https://doi.org/10.1016/j.nima.2011.10.018
15. J. Scherr, P. Tsvetkov, Design strategies for LWR and VHTR test environments in a fast spectrum reactor. Ann. Nucl. Energy **120**, 219–235 (2018). https://doi.org/10.1016/j.anucene.2018.05.046
16. C. Cao, Q. Gan, An adaptive optimization reverse regulation method for neutron spectrum based on standardized response module. Fusion Eng. Des. **163**, 112155 (2021). https://doi.org/10.1016/j.fusengdes.2020.112155
17. S. Mirjalili, *Evolutionary Algorithms and Neural Networks. Studies in Computational Intelligence*, vol. 780 (Springer, Cham, 2019). https://doi.org/10.1007/978-3-319-93025-1_4
18. D. Li, Q. Pan, X. Liu, High-resolution rapid calculation method of neutron spectrum based on energy response. Nucl. Eng. Technol. **57**(7), 103490 (2025). https://doi.org/10.1016/j.net.2025.103490
19. M. Filippo, J. Krepel, K. Mikityuk et al., Analysis of major group structures used for nuclear reactor simulations, in *Proceedings of the 26th International Conference on Nuclear Engineering,* July 22–26 London, UK (2018). https://doi.org/10.1115/ICONE26-81445
20. D. She, K. Wang, G. Yu, Development of the point-depletion code DEPTH. Nucl. Eng. Des. **258**, 235–240 (2023). https://doi.org/10.1016/j.nucengdes.2013.01.007
21. G. Sun, M. Cheng, Development of a MCNP and ORIGEN2 based burnup code for molten salt reactor. Nucl. Sci. Tech. **27**, 65 (2016). https://doi.org/10.1007/s41365-016-0070-1
22. S. Hogle, G.I. Maldonado, Modeling of the high flux isotope reactor cycle 400 with KENO-VI. Trans. Am. Nucl. Soc. **104**, 915–917 (2011).
23. K. Wang, Z. Li, D. She et al., RMC—A Monte Carlo code for reactor core analysis. Ann. Nucl. Energy **82**, 121–129 (2015). https://doi.org/10.1016/j.anucene.2014.08.048
24. T. Huang, Z. Li, K. Wang et al., Hybrid windowed networks for on-the-fly Doppler broadening in RMC code. Nucl. Sci. Tech. **32**(6), 62 (2021). https://doi.org/10.1007/s41365-021-00901-2
25. Z. Li, K. Wang, Y. Guo et al., Forced propagation method for Monte Carlo fission source convergence acceleration in the RMC. Nucl. Sci. Tech. **32**, 27 (2021). https://doi.org/10.1007/s41365-021-00868-0
26. D. Chandler, B. Betzler, G. Hirtz et al., Modeling and depletion simulations for a high flux isotope reactor cycle with a representative experiment loading. Oak Ridge National Laboratory, United States (2016). https://doi.org/10.2172/1325434
27. F. Peng, S. Liu, B. Wei et al., Simulation and experimental study of a random neutron analyzing system with ^{252}Cf neutron source.

Nucl. Sci. Tech. **22**(1), 39–46 (2011). https://doi.org/10.13538/j.1001-8042/nst.22.39-46
28. A. Shmelev, N. Geraskin, G. Kulikov et al., The problem of large-scale production of plutonium-238 for autonomous energy sources. J. Phys. Conf. Ser. **1689**, 012030 (2020). https://doi.org/10.1088/1742-6596/1689/1/012030
29. J. Cai, D. Li, P. Wang et al., Fast pulse sampling module for real-time neutron-gamma discrimination. Nucl. Sci. Tech. **30**, 84 (2019). https://doi.org/10.1007/s41365-019-0595-1
30. C. Daily, J. McDuffee, Design studies for the optimization of ^{238}Pu production in NpO_2 targets irradiated at the high flux isotope reactor. Nucl. Technol. **206**, 1182–1194 (2020). https://doi.org/10.1080/00295450.2019.1674594
31. Z. Fang, M. Yu, Y. Huang et al., Theoretical analysis of long-lived radioactive waste in pressurized water reactor. Nucl. Sci. Tech. **32**, 72 (2021). https://doi.org/10.1007/s41365-021-00911-0

Publisher's Note Springer Nature remains neutral with regard to jurisdictional claims in published maps and institutional affiliations.

Springer Nature or its licensor (e.g. a society or other partner) holds exclusive rights to this article under a publishing agreement with the author(s) or other rightsholder(s); author self-archiving of the accepted manuscript version of this article is solely governed by the terms of such publishing agreement and applicable law.